



# An Analytic Element Model for Seepage Forces in Fractured Media

Erik A. L. Toller<sup>1,2</sup> · Otto D. L. Strack<sup>3</sup>

Received: 30 January 2024 / Accepted: 18 April 2024 / Published online: 9 May 2024  
© The Author(s) 2024

## Abstract

There are many situations where groundwater flow has high flow rates, causing large seepage forces. Examples are flows around highly conductive fractures and tunnels. We present a new analytic element for a tunnel in an elastic medium. We combined the analytic element method for groundwater flow with that for linear elasticity, and include the seepage force as a body force in the linearly elastic model. We represent tunnels and fractures as analytic elements. The solution for the case considered is limited to steady state flow and fluid-to-solid coupling. We present examples of the computed seepage forces around a tunnel and a fracture as well as a comparison with another numerical model.

**Keywords** Analytic element method · Linear elasticity · Seepage forces · Tunnels · Fractures · Complex variables

**Mathematics Subject Classification** 30K15 · 74B05 · 30C20

## 1 Introduction

Flowing groundwater exerts a force, the seepage force, which is proportional to the gradient of the hydraulic head, which may cause a loss of stability if the gradient is large. High gradients occur near tunnels; their draining effect increases if highly conductive fractures are nearby.

We handle seepage forces by considering groundwater flow and linear elasticity as a coupled process, which can either be coupled in one way or in two ways [16]. [10], and [17] state that there exist four types of couplings between rock and groundwater that can be divided into two types, direct and indirect. We consider a fluid-to-solid coupling where the seepage forces affect the stresses and strains but not the reverse. We limit the analysis to fractures and tunnels.

---

✉ E.A.L. Toller  
[erik.toller@geo.uu.se](mailto:erik.toller@geo.uu.se); [erik.toller@wsp.com](mailto:erik.toller@wsp.com)

<sup>1</sup> Department of Earth Sciences, Uppsala University, Villavägen 16, 752 36, Uppsala, Sweden

<sup>2</sup> WSP Sverige AB, Stockholm, Sweden

<sup>3</sup> Department of Civil, Environmental, and Geo- Engineering, University of Minnesota, Minnesota, USA

Numerous formulations exist for the effect of seepage forces on the stability of a tunnel face. [2] used a limit equilibrium method which was later improved by [9]. [7] included the seepage force as a body force acting on the rock mass in three dimensions. Furthermore, [7] employed a numerical model for the groundwater flow and implemented the interpolated hydraulic head in a kinematical approach of limit analysis. [8] present an analytic description of the seepage forces on a circular tunnel, for both zero pressure and constant head along the tunnel lining. [8] mapped the half-space with a circular tunnel onto a disk in a transformed plane. The analytic solution they present applies to steady state and shows that the seepage force on the tunnel lining greatly increases with the tunnel depth.

When considering the combined effect of seepage forces and pressurized fractures, it is common to study fracture propagation. Some consider only the flow within the fracture, e.g. [5], while others study the fracture and seepage, e.g. [18]. [19] studied seepage forces in a fractured rock system with water injection. [19] show how the seepage forces vary over time and how they propagate around fractures. As expected, the seepage force is high close to fractures that draw water from the rock matrix. [4] and [3] studied the effects of loading a pressurized fracture on the normal stress and the pore pressure. Accounting for the pressure in both the pore space and the fracture, they studied the transient effects on the stress intensity factor and the fluid leak-off.

The objective of this paper is to further develop the linear elastic analytic element model developed by [13] and [14] to include the body force due to seepage and to develop the analytic element for a tunnel in a linearly elastic medium in plane strain. The main objective is to create an analytic element model that couples the groundwater flow model with the linearly elastic one. This results in a model where the seepage forces are known at every point in the medium, allowing us to investigate with high resolution the behavior at points in the vicinity of singularities. It also allows us to investigate the importance of seepage forces on tunnels relative to the effect of gravity. The model has no theoretical limit on the number of elements that can be included.

We consider the components of the contributions of the seepage force to both the displacement vector and the stress tensors, using the terms for a body force in the governing equation. We include the gravitational body force in the same terms. We express the seepage force in terms of the complex discharge potential obtained from the groundwater model. We assume that the groundwater model is not affected by the elastic deformations, so that the complex discharge potential remains fixed throughout the domain. This assumption does not limit us in our primary engineering objective, determining the importance of the effect of flow singularities on the stability of tunnel walls. The effect of the flow singularities on the stresses in the tunnel wall appears, somewhat surprisingly, to be minor.

We present solutions for tunnels, single and intersecting fractures; first separately for flow and deformations and then combined, using superposition. We observe the impact of seepage forces near singular points and as a function of distance to the element. We use this to determine where seepage forces should be considered and how much impact they have depending on the situation. A comparison of the simulated seepage forces from the presented AEM model and a COMSOL Multiphysics® model is presented for a case of a tunnel in fractured rock.

## 2 Equations for Linear Elasticity

We follow the notation in [13] for linear elasticity with body forces for the displacement vector and stress tensor in terms of complex functions  $\Phi$  and  $\Psi$  and the body force  $B_1$  and

$B_2$ . The complex displacement for linear elasticity with body forces is:

$$w = u_x - iu_y = \frac{1}{4G} \left\{ -\bar{z}\Phi'(z) + \kappa\bar{\Phi}(\bar{z}) + \Psi(z) - 2(1 - 2\nu)\bar{B}_2(\bar{z}) \right\} \tag{1}$$

where  $z = x + iy$ , and  $u_x$  and  $u_y$  are the components of the displacement vector in Cartesian  $(x, y)$ -space. We express the contra-variant components of the stress tensor in non-Cartesian  $(\bar{z}, z)$ -space as:

$$\tau^{11} = \bar{z}\Phi''(z) - \Psi'(z) \tag{2}$$

and

$$\tau^{12} = -\Phi'(z) - \bar{\Phi}'(\bar{z}) + \bar{B}_1(\bar{z}) + B_1(z). \tag{3}$$

The expressions for  $\tau^{11}$  and  $\tau^{12}$  in terms of the Cartesian components,  $\sigma_{xx}$ ,  $\sigma_{xy}$ , and  $\sigma_{yy}$ , of the stress tensor are

$$\tau^{11} = \sigma_{xx} - \sigma_{yy} - 2i\sigma_{xy} \tag{4}$$

and

$$\tau^{12} = \sigma_{xx} + \sigma_{yy}. \tag{5}$$

[13] presents expressions for the traction components in terms of  $\tau^{11}$  and  $\tau^{12}$  along a plane at an angle  $\alpha$  to the  $x$ -axis:

$$t_s - it_n = -\frac{1}{2}i \left[ \tau^{11}e^{2i\alpha} - \tau^{12} \right]. \tag{6}$$

### 3 The Body Force

The body force consists of the seepage force plus gravity. The components of the seepage force are

$$s_x = -\rho_w g \frac{\partial \phi}{\partial x}, \quad s_y = -\rho_w g \frac{\partial \phi}{\partial y}, \tag{7}$$

where  $\rho_w$  is the density of water,  $g$  is the gravitational acceleration and  $\phi$  is the hydraulic head. We write the seepage force in complex form as

$$S = s_x - is_y = -\rho_w g \left( \frac{\partial \phi}{\partial x} - i \frac{\partial \phi}{\partial y} \right) = -2\rho_w g \frac{\partial \phi}{\partial z}. \tag{8}$$

We obtained the trailing expression from the chain rule and  $\partial x/\partial z = 1/2$ ,  $\partial y/\partial z = 1/(2i)$ . We express the complex body force  $B_0$  in terms of its Cartesian components:

$$B_0 = \beta_x - i\beta_y, \tag{9}$$

and add to  $\beta_y$  the contribution of gravity,

$$B_0 = i\rho g - 2\rho_w g \frac{\partial \phi}{\partial z}. \tag{10}$$

We follow [12] and restrict the groundwater flow to divergence-free irrotational flow, so that  $\phi$  is a harmonic function of position that we write as the real part of a complex potential,  $\Omega^*$ ,

$$2 \frac{\partial \phi}{\partial z} = \frac{1}{k} \frac{d\Omega^*}{dz} \tag{11}$$

and

$$B_0 = i\rho g - \frac{\rho_w g}{k} \frac{d\Omega^*}{dz}. \tag{12}$$

We introduce a holomorphic complex potential  $\Omega$  that represents both the gravity and seepage forces:

$$\Omega = i\rho g z - \frac{\rho_w g}{k} \Omega^* = \rho g \left[ iz - \frac{\rho_w}{\rho} \frac{1}{k} \Omega^* \right], \tag{13}$$

where  $\Omega$  is a function of  $z$  only, i.e., does not depend on  $\bar{z}$ . We write (10) as

$$B_0 = \frac{d\Omega}{dz} = \rho g \left[ i - \frac{\rho_w}{\rho} \frac{1}{k} \frac{d\Omega^*}{dz} \right], \tag{14}$$

and integrate to obtain an expression for  $B_1$ :

$$B_1 = \rho g \left[ iz - \frac{\rho_w}{\rho} \frac{1}{k} \Omega^* \right] = \Omega. \tag{15}$$

We integrate again for  $B_2$

$$B_2 = \int \Omega dz = \rho g \left[ \frac{1}{2} iz^2 - \frac{\rho_w}{\rho} \frac{1}{k} \int \Omega^* dz \right]. \tag{16}$$

The body forces are included in the global component of the traction rather than in individual analytic elements.

## 4 An Analytic Element for a Circular Tunnel

We derive the expression for an analytic element for a circular tunnel with a constant atmospheric pressure acting against its wall. We present the analytic element for a constant pressure tunnel for groundwater flow in Appendix A. The tunnel is in an infinite domain, has a radius  $r_t$ , and is centered at  $z_t$ . We create the analytic element such that it can be combined with other analytic elements.

### 4.1 The Traction

Both traction components are zero along the tunnel wall so that the two components of the transformed stress tensor,  $\tau^{11}$  and  $\tau^{12}$ , are zero as well. The other two components of the stress tensor are the complex conjugates of the first two and need not be considered. The

latter tensor components are given by (2) and (3). We replace the body force  $B_1(z)$  in (3) by  $\Omega(z)$ :

$$\tau^{12} = -[\Phi'(z) + \bar{\Phi}'(\bar{z})] + \bar{\Omega}(\bar{z}) + \Omega(z). \tag{17}$$

The complex potential  $\Omega$  is the sum of the gravitational and seepage forces. We introduce a dimensionless variable  $Z = X + iY$ :

$$Z = \frac{z - z_t}{r_t} \tag{18}$$

with its inverse

$$z = Zr_t + z_t, \tag{19}$$

and express  $\tau^{11}$  in terms of  $Z$ :

$$\tau^{11} = \bar{Z}r_t\Phi''(z) + \bar{z}_t\Phi''(z) - \Psi'(z). \tag{20}$$

We introduce a function  $\Psi(z)$  via its derivative as

$$\Psi'(z) = \left[\frac{r_t}{Z} + \bar{z}_t\right]\Phi''(z) + \psi'(z), \tag{21}$$

and include this in the expression for  $\tau^{11}$

$$\tau^{11} = \bar{Z}r_t\Phi''(z) + \bar{z}_t\Phi''(z) - \frac{r_t}{Z}\Phi''(z) - \bar{z}_t\Phi''(z) - \psi'(z) \tag{22}$$

or

$$\tau^{11} = r_t \left(\bar{Z} - \frac{1}{Z}\right)\Phi''(z) - \psi'(z). \tag{23}$$

We use (6) to write the traction components in terms of  $\tau^{11}$  and  $\tau^{12}$ . The first term in (23) vanishes, because  $Z\bar{Z} = 1$  along the boundary of the tunnel,

$$t_s - it_n = -\frac{1}{2}i[-\psi'(z)e^{2i\alpha} + \Phi'(z) + \bar{\Phi}'(\bar{z}) - (\Omega(z) + \bar{\Omega}(\bar{z}))], \quad Z\bar{Z} = 1 \tag{24}$$

where  $\alpha$ , shown in Fig. 1, is the angle between an increment  $dZ$  that points in a counter-clockwise direction along the tunnel wall;  $\alpha = \theta + \pi/2$  so that, with  $Z = e^{i\theta}$

$$t_s - it_n = -\frac{1}{2}i[-\psi'(z)e^{2i\theta}e^{i\pi} + \Phi'(z) + \bar{\Phi}'(\bar{z}) - (\Omega(z) + \bar{\Omega}(\bar{z}))], \quad Z\bar{Z} = 1. \tag{25}$$

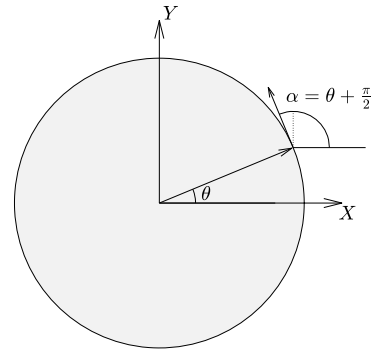
$Z$  is a point on the circle;  $e^{2i\alpha} = e^{2i\theta+i\pi} = -Z^2$ , and

$$t_s - it_n = -\frac{1}{2}i[\psi'(z)Z^2 + \Phi'(z) + \bar{\Phi}'(\bar{z}) - (\Omega(z) + \bar{\Omega}(\bar{z}))], \quad Z\bar{Z} = 1. \tag{26}$$

We introduce a function  $\Xi$  as:

$$\Xi = \psi'(z)Z^2 \tag{27}$$

**Fig. 1** The angle  $\alpha$  along the tunnel wall



and use it in (26):

$$t_s - it_n = -\frac{1}{2}i [\Xi(z) + 2\Re\Phi'(z)] + \frac{1}{2}i[\Omega(z) + \bar{\Omega}(\bar{z})], \quad Z\bar{Z} = 1. \tag{28}$$

We introduce additional functions  $P(z)$  and  $Q(z)$ ,

$$\Re Q = \frac{1}{2}\Re \Xi + \Re \Phi' \tag{29}$$

and

$$\Im P = \frac{1}{2}\Im \Xi. \tag{30}$$

We use (28) to express the tractions in terms of  $Q$ ,  $P$  and  $\Omega$

$$t_s - it_n = -i\Re Q(z) + \Im P(z) + \frac{1}{2}i[\Omega(z) + \bar{\Omega}(\bar{z})], \quad Z\bar{Z} = 1 \tag{31}$$

or

$$\Im P = t_s, \quad Z\bar{Z} = 1 \tag{32}$$

and

$$\Re Q = t_n + \frac{1}{2}[\Omega(z) + \bar{\Omega}(\bar{z})], \quad Z\bar{Z} = 1. \tag{33}$$

The functions  $P(z)$  and  $Q(z)$  are holomorphic outside the unit circle; we expand each in terms of an asymptotic series:

$$P = \sum_{n=0}^{\infty} a_n Z^{-n}, \quad Z\bar{Z} = 1 \tag{34}$$

and

$$Q = \sum_{n=0}^{\infty} b_n Z^{-n}, \quad Z\bar{Z} = 1. \tag{35}$$

We determine the unknown coefficients from the conditions that the tractions due to both the tunnel element and the other elements are zero along the tunnel wall.

We follow an approach similar to that explained in [12]. We use the functions  $P$  and  $Q$  to create shear and normal tractions along the tunnel wall that cancel the values contributed by the other elements. We employ the method of holomorphic matching explained in [11] to determine the coefficients  $a_n$  and  $b_n$  in (34) and (35). Through holomorphic matching, we derive a relationship between the unknown coefficients  $a_n$  and  $b_n$  and a set of known coefficients given by a holomorphic function that is represented by its own Taylor series. Although an arbitrary function such as  $t_s$  or  $t_n$ , cannot be written in terms of a single complex variable everywhere, it can be done along a single line or curve. The method of achieving this is holomorphic matching.

The tractions  $t_s$  and  $t_n$  are not harmonic functions and cannot be represented in terms of real or imaginary parts of the complex Taylor series. However, the expressions for  $t_s$  and  $t_n$  do not have singularities inside the circular tunnel boundary. Therefore  $t_s$  and  $t_n$  can each be viewed as the boundary values of some holomorphic function. We represent these functions as  $R$  and  $S$ , with

$$t_{s, \text{ other}} = \Im R(Z), \quad Z\bar{Z} = 1 \tag{36}$$

and

$$t_{n, \text{ other}} = \Re S(Z), \quad Z\bar{Z} = 1. \tag{37}$$

The components of the body forces are included in the expression for  $t_{n, \text{ other}}$ . We expand both  $R$  and  $S$  in terms of a Taylor series about  $Z = 0$ ,

$$R = \sum_{n=0}^{\infty} \lambda_n Z^n \tag{38}$$

and

$$S = \sum_{n=0}^{\infty} \mu_n Z^n. \tag{39}$$

We use Cauchy integrals to determine  $\lambda_n$  and  $\mu_n$ :

$$\lambda_n = \frac{i}{\pi} \int_0^{2\pi} t_{s, \text{ other}} e^{-in\theta} d\theta \tag{40}$$

and

$$\mu_n = \frac{1}{\pi} \int_0^{2\pi} t_{n, \text{ other}} e^{-in\theta} d\theta. \tag{41}$$

Representing  $t_s$  and  $t_n$  as these series is valid only along the boundary  $Z\bar{Z} = 1$ .

We express  $t_s$  as the real part of  $R$ ,

$$t_{s, \text{ other}} = \frac{1}{2i} \sum_{n=0}^{\infty} [\lambda_n Z^n - \bar{\lambda}_n \bar{Z}^n]. \tag{42}$$

The shear stress due to the combination of the tunnel element and the other elements must vanish for  $Z\bar{Z} = 1$ :

$$t_s = \frac{1}{2i} \sum_{n=0}^{\infty} [\lambda_n Z^n - \bar{\lambda}_n \bar{Z}^n + a_n Z^{-n} - \bar{a}_n \bar{Z}^{-n}] = 0, \quad Z\bar{Z} = 1. \tag{43}$$

We apply holomorphic matching along the tunnel wall by replacing the non-holomorphic term  $\bar{Z}$  by  $1/Z$ :

$$t_s = 0 = \frac{1}{2i} \sum_{n=0}^{\infty} [(\lambda_n - \bar{a}_n)Z^n + (a_n - \bar{\lambda}_n)Z^{-n}]. \tag{44}$$

This condition is satisfied if, for all  $n$ ,

$$\lambda_n = \bar{a}_n \quad n = 0, 1, \dots, \infty. \tag{45}$$

We apply a similar approach to  $t_n$ , which gives

$$\mu_n = -\bar{b}_n \quad n = 0, 1, \dots, \infty. \tag{46}$$

We express the functions involved in the tunnel element in terms of  $P$ ,  $Q$ , and  $\Omega$ . We apply (30) to determine  $\Xi$  from

$$\Im P = \frac{1}{2i} (P - \bar{P}) = \frac{1}{4i} (\Xi - \bar{\Xi}), \tag{47}$$

so that:

$$\Xi = 2P. \tag{48}$$

We use (29) to obtain an expression with  $\Phi'$ :

$$\Re Q = \frac{1}{2} (Q + \bar{Q}) = \frac{1}{4} (\Xi + \bar{\Xi}) + \frac{1}{2} (\Phi' + \bar{\Phi}') \tag{49}$$

or

$$\Phi' = Q - P, \tag{50}$$

so that

$$\Phi' = Q - P = \sum_{n=0}^{\infty} (b_n - a_n) Z^{-n}. \tag{51}$$

We find  $\psi'$  from (27)

$$\psi' = 2PZ^{-2} = 2 \sum_{n=0}^{\infty} a_n Z^{-(n+2)}. \tag{52}$$

We use

$$\frac{dZ}{dz} = \frac{1}{r_t} \tag{53}$$



when differentiating  $\Phi'$  with respect to  $Z$ ,

$$\Phi'' = -\frac{1}{r_t} \sum_{n=0}^{\infty} n(b_n - a_n)Z^{-(n+1)}. \tag{54}$$

### 4.2 The Displacements

The equation for complex displacement is given in (1). A constant,  $w_\infty$ , can be added such that the displacements are symmetrical relative to the origin. We integrate  $\Psi'$ :

$$\Psi = \int \frac{r_t}{Z} \Phi'' dz + \bar{z}_t \Phi' + \psi, \tag{55}$$

where

$$\int \frac{r_t}{Z} \Phi'' dz = - \int \sum_{n=0}^{\infty} n(b_n - a_n)Z^{-(n+2)} dz = \sum_{n=0}^{\infty} n \frac{b_n - a_n}{n + 1} Z^{-(n+1)} \tag{56}$$

and

$$\psi = -2 \sum_{n=0}^{\infty} \frac{a_n}{n + 1} Z^{-(n+1)}. \tag{57}$$

We integrate  $\Phi'$  as well

$$\Phi = r_t \left[ (b_0 - a_0)Z + (b_1 - a_1) \ln(Z) + \sum_{n=2}^{\infty} \frac{b_n - a_n}{1 - n} Z^{-(n-1)} \right]. \tag{58}$$

## 5 An Analytic Element for a Fracture in Groundwater Flow

We modify the analytic element function for a fracture/crack, presented in [14] to include body forces. A more extensive derivation of the resulting stress tensor is in [14].

### 5.1 The Traction

We write the expression for the stress tensor components for a fracture at an angle  $\gamma$  and of length  $L$  as

$$\tau^{11} = -\frac{1}{2}L(Z - \bar{Z})\phi''(z) - e^{-i\gamma}\phi'(z) - e^{-i\gamma}\psi'(z) \tag{59}$$

and

$$\tau^{12} = -e^{i\gamma}\phi'(z) - e^{-i\gamma}\bar{\phi}'(\bar{z}) + (\bar{\Omega}(\bar{z}) + \Omega(z)), \tag{60}$$

where, as in [14] (equations: (27) and (28)),  $\phi = e^{-i\gamma} \Phi$ . The real part of the complex potential, and thus the hydraulic head, is in the expression for  $\tau^{12}$  and directly affects the isotropic stress. The traction along the element is

$$T^1_\gamma = t_s - it_n = -\frac{1}{2}i[\tau^{11}e^{2i\gamma} - \tau^{12}]. \tag{61}$$

We use (59) and (60):

$$t_{\frac{s}{\gamma}} - it_{\frac{n}{\gamma}} = -\frac{1}{2}i \left[ \left( -\frac{1}{2}L(Z - \bar{Z})\phi''(z) - e^{-i\gamma}\phi'(z) - e^{-i\gamma}\psi'(z) \right) e^{2i\gamma} \right. \\ \left. + e^{i\gamma}\phi'(z) + e^{-i\gamma}\bar{\phi}'(\bar{z}) - (\bar{\Omega}(\bar{z}) + \Omega(z)) \right], \tag{62}$$

where  $Z = \bar{Z}$  along the element, so that

$$t_{\frac{s}{\gamma}} - it_{\frac{n}{\gamma}} = \frac{1}{2}i \left[ e^{i\gamma}\phi'(z) + e^{i\gamma}\psi'(z) - e^{i\gamma}\phi'(z) - e^{-i\gamma}\bar{\phi}'(\bar{z}) + (\bar{\Omega}(\bar{z}) + \Omega(z)) \right] \tag{63}$$

or

$$t_{\frac{s}{\gamma}} - it_{\frac{n}{\gamma}} = \frac{1}{2}i \left[ e^{i\gamma}\psi'(z) - e^{-i\gamma}\bar{\phi}'(\bar{z}) + (\bar{\Omega}(\bar{z}) + \Omega(z)) \right]. \tag{64}$$

We write the functions  $\phi$  and  $\psi$  in terms of asymptotic expansions, which converge outside the unit circle in the  $\chi$ -plane:

$$\phi = \sum_{n=1}^{\infty} \alpha_n \chi^{-n}, \tag{65}$$

$$\psi = \sum_{n=1}^{\infty} \beta_n \chi^{-n}. \tag{66}$$

The derivative of these equations are in [14], and are

$$\phi' = \frac{d\phi}{dz} = -\sum_{n=1}^{\infty} n\alpha_n \frac{\chi^{-(n-1)}}{\chi^2 - 1} \frac{4}{L} e^{-i\gamma}, \tag{67}$$

$$\psi' = \frac{d\psi}{dz} = -\sum_{n=1}^{\infty} n\beta_n \frac{\chi^{-(n-1)}}{\chi^2 - 1} \frac{4}{L} e^{-i\gamma}, \tag{68}$$

and

$$\phi'' = \frac{d^2\phi}{dz^2} = \sum_{n=1}^{\infty} n\alpha_n \frac{16}{L^2} e^{-2i\gamma} \frac{\chi^{2-n}}{(\chi^2 - 1)^3} [(n + 1)\chi^2 - n + 1]. \tag{69}$$

We insert these in (64),

$$t_{\frac{s}{\gamma}} - it_{\frac{n}{\gamma}} = -\frac{1}{2}i \left[ e^{i\gamma} \left( \sum_{n=1}^{\infty} n\beta_n \frac{\chi^{-(n-1)}}{\chi^2 - 1} \frac{4}{L} e^{-i\gamma} \right) \right. \\ \left. - e^{-i\gamma} \left( \sum_{n=1}^{\infty} n\bar{\alpha}_n \frac{\bar{\chi}^{-(n-1)}}{\bar{\chi}^2 - 1} \frac{4}{L} e^{i\gamma} \right) - (\bar{\Omega}(\bar{z}) + \Omega(z)) \right], \tag{70}$$

and simplify to give

$$t_{\gamma} - it_n = -\frac{1}{2}i \left[ \frac{4}{L} \sum_{n=1}^{\infty} \left( n\beta_n \chi^{-n} \frac{\chi}{\chi^2 - 1} - n\bar{\alpha}_n \bar{\chi}^{-n} \frac{\bar{\chi}}{\bar{\chi}^2 - 1} \right) - (\bar{\Omega}(\bar{z}) + \Omega(z)) \right]. \tag{71}$$

We have  $\chi \bar{\chi} = 1$  along the crack,

$$\frac{\bar{\chi}}{\bar{\chi}^2 - 1} = \frac{\chi}{1 - \chi^2} = -\frac{\chi}{\chi^2 - 1}, \tag{72}$$

which gives

$$t_{\gamma} - it_n = -\frac{1}{2}i \left[ \frac{4}{L} \frac{\chi}{\chi^2 - 1} \sum_{n=1}^{\infty} n (\beta_n \chi^{-n} + \bar{\alpha}_n \chi^n) \right] + \frac{1}{2}i(\bar{\Omega}(\bar{z}) + \Omega(z)). \tag{73}$$

### 5.2 Continuity of Tractions

As in [14] we use the condition of continuity of tractions; the tractions must be continuous across the fracture, to find  $\alpha_n$  and  $\beta_n$ :

$$\begin{aligned} t_{\gamma}^+ - it_n^+ - \left( t_{\gamma}^- - it_n^- \right) = \\ -\frac{1}{2}i \left\{ \left[ \frac{4}{L} \frac{\chi}{\chi^2 - 1} \sum_{n=1}^{\infty} n (\beta_n \chi^{-n} + \bar{\alpha}_n \chi^n) - (\bar{\Omega}(\bar{z}) + \Omega(z)) \right] \right. \\ \left. - \left[ \frac{4}{L} \frac{\bar{\chi}}{\bar{\chi}^2 - 1} \sum_{n=1}^{\infty} n (\beta_n \bar{\chi}^{-n} + \bar{\alpha}_n \bar{\chi}^n) - (\Omega(z) + \bar{\Omega}(\bar{z})) \right] \right\}, \quad \chi \bar{\chi} = 1. \end{aligned} \tag{74}$$

We simplify, using that  $\bar{\chi} = \chi^{-1}$ ,

$$\begin{aligned} \left[ \frac{4}{L} \frac{\chi}{\chi^2 - 1} \sum_{n=1}^{\infty} n (\beta_n \chi^{-n} + \bar{\alpha}_n \chi^n) - (\bar{\Omega}(\bar{z}) + \Omega(z)) \right] \\ + \left[ \frac{4}{L} \frac{\chi}{\chi^2 - 1} \sum_{n=1}^{\infty} n (\beta_n \chi^n + \bar{\alpha}_n \chi^{-n}) + (\bar{\Omega}(\bar{z}) + \Omega(z)) \right], \quad \chi \bar{\chi} = 1, \end{aligned} \tag{75}$$

and combine terms:

$$\frac{4}{L} \frac{\chi}{\chi^2 - 1} \sum_{n=1}^{\infty} n \{ \beta_n (\chi^n + \chi^{-n}) + \bar{\alpha}_n (\chi^n + \chi^{-n}) \}. \tag{76}$$

The tractions are continuous across the crack, provided that

$$\alpha_n = -\bar{\beta}_n. \tag{77}$$

The relationship between  $\alpha_n$  and  $\beta_n$  is identical to that in [14]. The normal traction  $t_n$  is also a function of the body force (73), but otherwise the solution for  $\beta_n$  is the same. We follow

**Table 1** General properties for rock mass and groundwater

$k$	=	$10^{-7}$	m/day, hydraulic conductivity of rock
$T = k_b b$	=	$10^{-3}$	$m^2$ /day, transmissivity of fractures
$\rho$	=	2520	kg/m <sup>3</sup> , density of rock
$\rho_w$	=	1000	kg/m <sup>3</sup> , density of water

[14] and express the unknown coefficients along the unit circle, using  $\chi = e^{i\theta}$ , as:

$$t_{\gamma} = -\frac{2}{L \sin(\theta)} \sum_{n=1}^{\infty} n \Im \beta_n \sin(n\theta) \tag{78}$$

and

$$t_n = -\frac{2}{L \sin(\theta)} \sum_{n=1}^{\infty} n \Re \beta_n \sin(n\theta). \tag{79}$$

The body forces are included in the contribution of all the other elements on  $t_n$ .

The value for the hydraulic pressure  $p$  in the fracture is given by the groundwater pressure

$$p = (\phi - \Im z) \rho_w g. \tag{80}$$

The complex potential  $\Omega^*$  is given by either the exact solution of flow with a single fracture or [15] for intersecting fractures. In order to plot the displacements please use the integral of the complex potential for intersecting fractures, from [15], in Appendix B.

### 6 Results

The general properties chosen for the rock mass and groundwater are given in Table 1; the values are based on [6] and [20].

We present in Fig. 2 the effect of the two components of the body force on the isotropic stress  $\tau^{12}$  as a function of depth. We also present the flow net for a tunnel at a given depth in a field of vertically downward uniform flow. For this and all other flow nets, the blue lines represent the stream lines, and the red lines the equipotentials. There is a branch cut because there is a net flow into the tunnel represented by the logarithm of the tunnel element, which causes a horizontal discontinuity in the stream function. The values of the two components of the body force are the mean values along the tunnel wall. We observe that the effect of gravity is consistently higher than that of the seepage force and this effect increases with the depth of the tunnel. When considering large depths the seepage force is negligible compared to gravity.

We plot in Fig. 3 the flow net for a fracture in uniform flow and the effect of the two components of the body force on the isotropic stress  $\tau^{12}$  as a function of distance in terms of fracture length projected onto the  $x$ -axis, beginning the plot at from the upper right fracture tip. We added a constant hydraulic head to the groundwater solution, a situation that could occur for a fracture beneath a lake. As mentioned, a constant head adds a constant component to the isotropic stress. We observe that close to the fracture tip the contribution of the seepage force changes rapidly with position due to the large gradient, see the small box in Fig. 3 (right). Gravity force is a function of elevation plus a constant. The shape of the plot

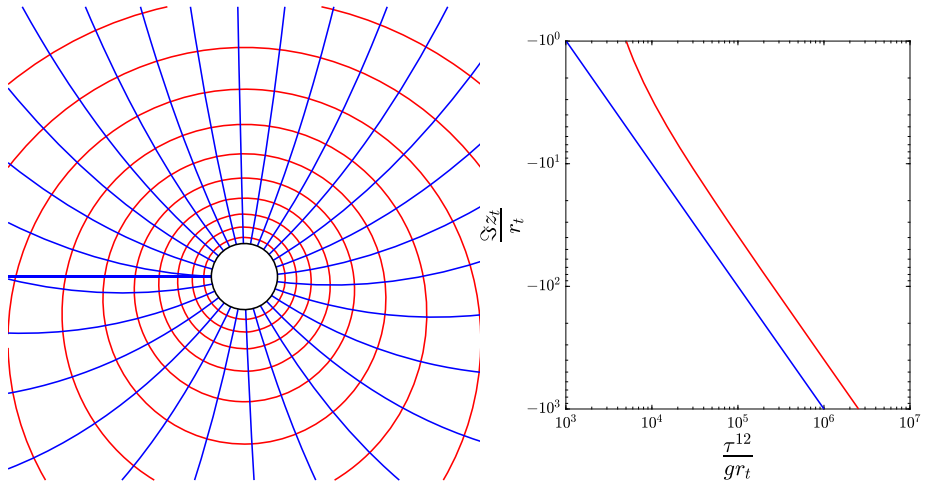


**Fig. 2** The flow net for a tunnel in a field of uniform flow (left) and the contribution of the two body force components, seepage force (blue) and gravity (red), on the isotropic stress as a function of depth (right)

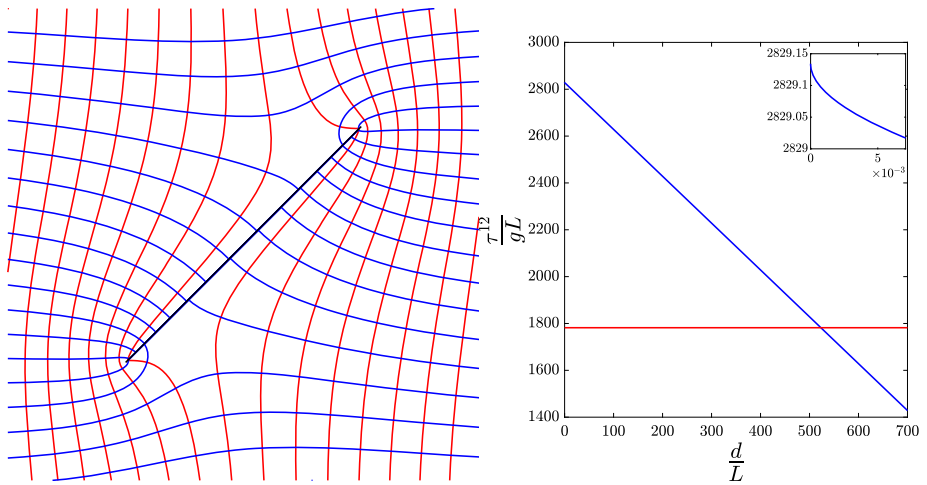


**Fig. 3** Flow net for a fracture in uniform flow (left) and the contribution of the two body force components, seepage force (blue) and gravity force (red), on the isotropic stress as a function of distance computed along a line parallel to the  $x$ -axis beginning at the upper right fracture tip parallel to the  $x$ -axis (right)

is highly dependent on the elevation of the fracture tip, the hydraulic head, and the uniform flow. For a case with a lower added hydraulic head or a lower fracture, gravity would be the dominating term. Contours of constant major principal stress are presented in Fig. 4.

We present a comparison between the presented AEM model and a COMSOL Multiphysics® model. The comparison concerns a tunnel in a fracture network under a constant gradient. The boundary conditions and flow net are presented in Fig. 5 and Table 1. To limit the far-field flow the model is bounded by a box that has two vertical impermeable sides and two horizontal constant head boundaries, each side is 500 m away from the tunnel

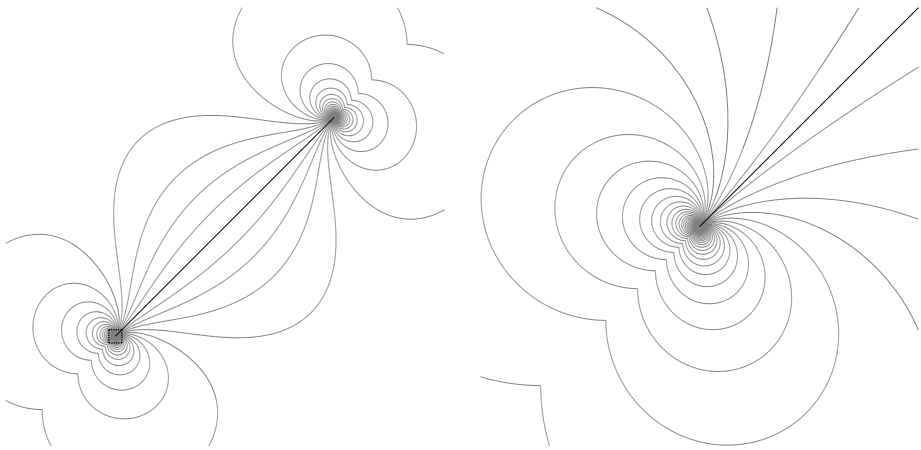


**Fig. 4** Contours of constant major principal stress for the fracture presented in Fig. 3 (left) and a zoomed plot for the area bounded by the dotted line on the left panel (right)

center. The tunnel has a radius of 7 m and a zero hydraulic head along the tunnel wall. The COMSOL Multiphysics<sup>®</sup> model simulates the groundwater flow using finite elements, based on Darcy's law [1]; the seepage force is calculated using (7). As for the AEM model, the flow in the COMSOL Multiphysics<sup>®</sup> model is calculated at steady state conditions prior to the calculation of the seepage force. The comparison of the seepage forces along the tunnel wall for the two models is presented in Fig. 6.

The relative difference between the two models is calculated using

$$\Delta s_j = \left| \frac{s_{j,\text{AEM}} - s_{j,\text{COMSOL}}}{s_{j,\text{COMSOL}}} \right|, \quad (81)$$

where  $j = x, y$ , and  $s_{j,\text{AEM}}$  and  $s_{j,\text{COMSOL}}$  are the seepage forces in the AEM model and the COMSOL Multiphysics<sup>®</sup> model respectively. The results show that the difference is generally less than 0.1%. There are peaks in the relative difference where the seepage force is close to zero. This is because the AEM model is almost zero while the COMSOL Multiphysics<sup>®</sup> model is much higher, e.g. for  $\chi = e^{i\pi}$ :  $s_{y,\text{AEM}} \approx 0.22 \text{ N/m}^3$  and  $s_{y,\text{COMSOL}} \approx 2000 \text{ N/m}^3$ , which means that (81) is equal to one. This further demonstrates that the AEM model accurately simulates the seepage force.

The accuracy of the AEM model improves as the number of coefficients increases, as in [14] and [15]. Because the AEM model approaches the exact solution, the AEM model and the COMSOL Multiphysics<sup>®</sup> model will never agree exactly.

## 7 Conclusion

We developed an analytic element model capable of including seepage forces as a body force within a linearly elastic medium in plane strain. We computed the effects of both seepage force and gravity force in a single expression. We illustrate how the effect of seepage forces varies with distance from the element and how it behaves near singularities. These insights are important when considering the effect of seepage forces and deciding when to include them.

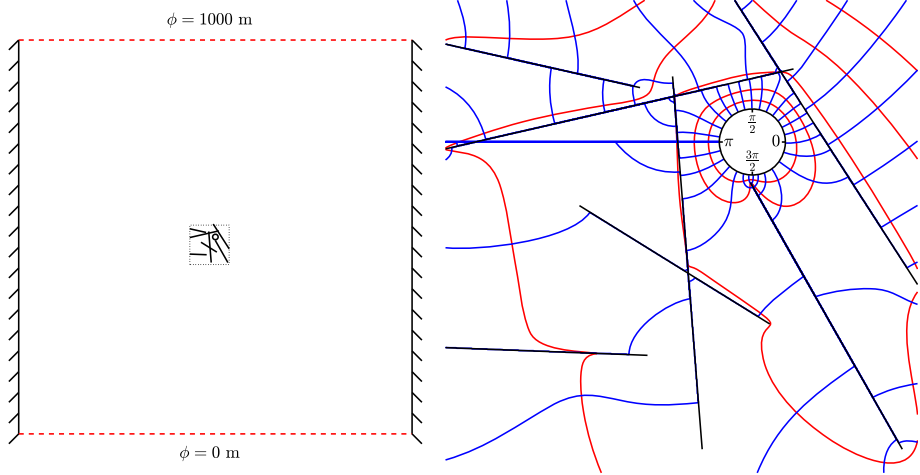


**Fig. 5** Illustration of the far field boundary conditions (left) and the flow net (right) for the area bounded by the dotted line on the left panel

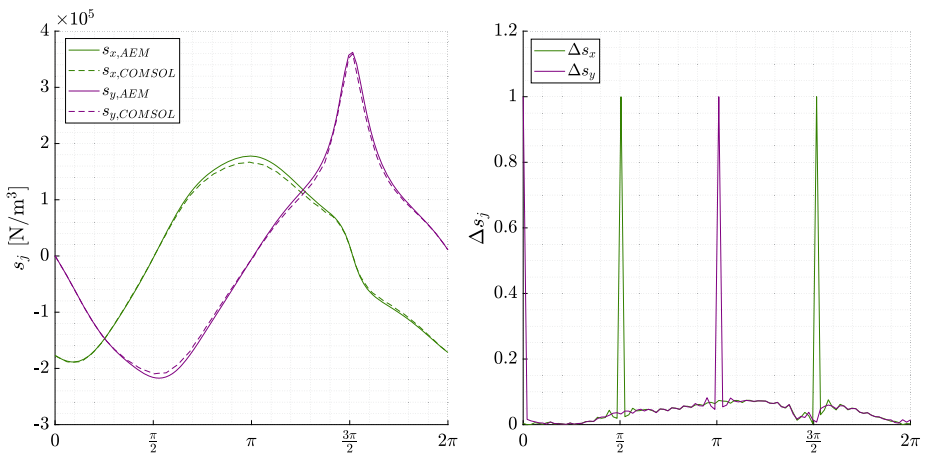


**Fig. 6** Comparison (left) and difference (right) of the computed seepage forces along the tunnel wall for the two models. The locations for  $0 \rightarrow 2\pi$  along the tunnel wall are marked on the right panel in Fig. 5

We compare the effect of seepage force and gravity. The effects of the two are highly dependent on both elevation and constant hydraulic head. Without an additional constant hydraulic head, gravity will in almost all cases be dominating.

We compared the presented model with a COMSOL Multiphysics® model and found that the difference between them is minimal. The difference in the compared case is less than 0.1%, except for points where the seepage force is close to zero. The results demonstrate that the presented model provides an accurate model for seepage forces.

We have shown that it is possible to combine the analytic element method for groundwater with that for linear elasticity. This hydro-mechanical model is limited to fluid-to-solid coupling and does not consider changes in the transmissivity of fractures due to stresses.

This limitation is acceptable as we limit the study to steady state conditions, and do not expect any changes in the groundwater properties after the steady state is reached.

### Appendix A: An Analytic Element for Flow to a Circular Tunnel with Constant Pressure

We consider a tunnel centered at  $z_t$  with a radius of  $r_t$ . We map the exterior of the tunnel onto the exterior of the unit circle in the  $Z$ -plane using

$$Z = \frac{z - z_t}{r_t}, \quad z = Zr_t + z_t. \tag{82}$$

We modify the analytic element for a constant head circular boundary from [12] and change it into a circular analytic element for a constant pressure. The complex discharge potential retains its form and is

$$\Omega^* = \sum_{n=1}^{\infty} c_n \frac{1}{Z^n} + \frac{Q}{2\pi} \ln\left(\frac{Z}{Z_{far}}\right) \tag{83}$$

where  $Z_{far}$  is the location of the reference point  $z_0$  in the  $Z$ -plane, i.e. the contribution from the discharge of the tunnel is zero at the reference point.

We solve for the unknown coefficients,  $c$ , using a Cauchy Integral

$$c_n = \frac{1}{\pi} \int_0^{2\pi} \Delta\Phi e^{-in\theta} d\theta \quad n = 1, \dots, \tag{84}$$

where

$$\Delta\Phi = \Phi_{other} - \Im\{z - z_t\}k \tag{85}$$

or

$$\Delta\Phi = \Phi_{other} - \sin(\theta)r_t k. \tag{86}$$

We integrate  $\Omega^*$  to get the components of  $B_2$ :

$$\Omega_1^* = \int \Omega^* dz = c_1 \ln(Z) + \sum_{n=2}^{\infty} c_n \frac{1}{1-n} \frac{1}{Z^{n-1}} + \frac{Q}{2\pi} \left[ Zr_t \ln\left(\frac{Z}{Z_{far}}\right) - z \right]. \tag{87}$$

### Appendix B: Integral of the Complex Potential for Flow with Intersecting Fractures

The integral of the complex potential, defined as  $\Omega_1^*$  is:

$$\Omega_1^* = \int \Omega^* dz = \int_{crack} \Omega^* \frac{dz}{dZ} \frac{dZ}{d\chi} d\chi + \int_{uni} \Omega^* dz, \tag{88}$$



where

$$\Omega_{\text{crack}}^* = \frac{1}{2\pi} \sum_{m=0}^M b_m F_m, \tag{89}$$

$$\frac{dz}{dZ} \frac{dZ}{d\chi} = e^{iy} \frac{L}{4} \left( 1 - \frac{1}{\chi^2} \right). \tag{90}$$

The far-field expansion of  $F_m$  is

$$F_m = \sum_{j=1}^{\infty} \alpha_j^m \frac{1}{\chi^j}. \tag{91}$$

We combine and integrate:

$$\begin{aligned} \int_{\text{crack}} \Omega^* dz &= \frac{L}{4} e^{iy} \int_{\text{crack}} \Omega^* \left( 1 - \frac{1}{\chi^2} \right) d\chi \\ &= \frac{L}{8\pi} e^{iy} \left[ \int \sum_{m=1}^M b_m \sum_{j=1}^{\infty} \alpha_j^m \frac{1}{\chi^j} \left( 1 - \frac{1}{\chi^2} \right) d\chi \right] \\ &= \frac{L}{8\pi} e^{iy} \left[ \int \sum_{m=1}^M b_m \sum_{j=1}^{\infty} \alpha_j^m \chi^{-j} d\chi - \int \sum_{m=1}^M b_m \sum_{j=1}^{\infty} \alpha_j^m \chi^{-(j+2)} d\chi \right] \\ &= \frac{L}{8\pi} e^{iy} \left[ \sum_{m=1}^M b_m \left( \alpha_1^m \ln(\chi) + \sum_{j=2}^{\infty} \alpha_j^m \frac{\chi^{-(j-1)}}{1-j} \right) \right. \\ &\quad \left. - \sum_{m=1}^M b_m \sum_{j=1}^{\infty} \alpha_j^m \frac{\chi^{-(j+1)}}{-(j+1)} \right]. \end{aligned} \tag{92}$$

We use the far-field expansion everywhere except for points on the element, where we use the near-field function

$$F_n = \left[ \chi^n + \frac{1}{\chi^n} \right] \ln \frac{\chi-1}{\chi+1} + 2\beta_n + 2 \sum_{j=1}^{n-1} \beta_{n-j} \left[ \chi^j + \frac{1}{\chi^j} \right]. \tag{93}$$

The integral of the uniform flow is

$$\int z W_{\text{uni}} dz = \frac{1}{2} z^2 W_{\text{uni}}. \tag{94}$$

**Acknowledgements** Many thanks to Dr. Liangchao Zou at the Royal Institute of Technology (Sweden) for providing us with the COMSOL Multiphysics® model.

**Author contributions** E.T. and O.S. wrote the manuscript and did the analysis. E.T. wrote the software and prepared the figures.

**Funding** Open access funding provided by Uppsala University. Dr. Erik A. L. Toller was funded by the Swedish Transport Administration Grant no. 7017.

**Data Availability** The code used for generating the results in this project is developed by the author Erik A. L. Toller and is preserved at <https://doi.org/10.5281/zenodo.10988574>.

## Declarations

**Competing interests** The authors declare no competing interests.

**Open Access** This article is licensed under a Creative Commons Attribution 4.0 International License, which permits use, sharing, adaptation, distribution and reproduction in any medium or format, as long as you give appropriate credit to the original author(s) and the source, provide a link to the Creative Commons licence, and indicate if changes were made. The images or other third party material in this article are included in the article's Creative Commons licence, unless indicated otherwise in a credit line to the material. If material is not included in the article's Creative Commons licence and your intended use is not permitted by statutory regulation or exceeds the permitted use, you will need to obtain permission directly from the copyright holder. To view a copy of this licence, visit <http://creativecommons.org/licenses/by/4.0/>.

## References

1. COMSOL AB (n.d.) Comsol multiphysics® v. 6.2. URL. [www.comsol.com](http://www.comsol.com)
2. Anagnostou, G., Kovári, K.: Face stability conditions with Earth-pressure-balanced shields. *Tunn. Undergr. Space Technol.* **11**(2), 165–173 (1996)
3. Detournay, E., Cheng, A.H.D.: Plane strain analysis of a stationary hydraulic fracture in a poroelastic medium. *Int. J. Solids Struct.* **27**(13), 1645–1662 (1991)
4. Detournay, E., Cheng, A.D., Roegiers, J.C., McLennan, J.: Poroelasticity considerations in situ stress determination by hydraulic fracturing. In: *International Journal of Rock Mechanics and Mining Sciences & Geomechanics Abstracts*, Elsevier, vol. 26, pp. 507–513 (1989)
5. Minkoff, S.E., Stone, C.M., Bryant, S., Peszynska, M., Wheeler, M.F.: Coupled fluid flow and geomechanical deformation modeling. *J. Pet. Sci. Eng.* **38**(1–2), 37–56 (2003)
6. Nordqvist, R., Gustafsson, E., Andersson, P., Thur, P.: Groundwater flow and hydraulic gradients in fractures and fracture zones at forsmark and oskarshamn. *Tech. Rep. SKB Rapport R-08-103*, Svensk Kärnbränslehantering AB, (2008)
7. Pan, Q., Dias, D.: Three dimensional face stability of a tunnel in weak rock masses subjected to seepage forces. *Tunn. Undergr. Space Technol.* **71**, 555–566 (2018)
8. Park, K.H., Lee, J.G., Owatsiriwong, A.: Seepage force in a drained circular tunnel: an analytical approach. *Can. Geotech. J.* **45**(3), 432–436 (2008)
9. Perazzelli, P., Leone, T., Anagnostou, G.: Tunnel face stability under seepage flow conditions. *Tunn. Undergr. Space Technol.* **43**, 459–469 (2014)
10. Rutqvist, J., Stephansson, O.: The role of hydromechanical coupling in fractured rock engineering. *Hydrogeol. J.* **11**, 7–40 (2003)
11. Strack, O.D.L.: Using Wirtinger calculus and holomorphic matching to obtain the discharge potential for an elliptical pond. *Water Resour. Res.* **45**(1) (2009)
12. Strack, O.D.L.: *Analytical Groundwater Mechanics*. Cambridge University Press, Cambridge (2017)
13. Strack, O.D.L.: *Applications of Vector Analysis and Complex Variables in Engineering*. Springer, Berlin (2020)
14. Strack, O.D.L., Toller, E.A.L.: An analytic element model for highly fractured elastic media. *Int. J. Numer. Anal. Methods Geomech.* **46**(2), 297–314 (2022)
15. Toller, E.A.L.: An analytic element model for intersecting and heterogeneous fractures in groundwater flow. *Water Resour. Res.* **58**(5), Article ID e2021WR031520 (2022)
16. Tsang, C.F.: *Coupled Processes Associated with Nuclear Waste Repositories*. Elsevier, Amsterdam (2012)
17. Wang, H.: *Theory of Linear Poroelasticity with Applications to Geomechanics and Hydrogeology*, vol. 2. Princeton University Press, Princeton (2000)
18. Yan, C., Zheng, H.: Fdem-flow3d: a 3d hydro-mechanical coupled model considering the pore seepage of rock matrix for simulating three-dimensional hydraulic fracturing. *Comput. Geotech.* **81**, 212–228 (2017)

19. Zhao, Y., Liu, Q., Zhang, C., Liao, J., Lin, H., Wang, Y.: Coupled seepage-damage effect in fractured rock masses: model development and a case study. *Int. J. Rock Mech. Min. Sci.* **144**, 104822 (2021)
20. Zimmerman, R.W., Bodvarsson, G.S.: Hydraulic conductivity of rock fractures. *Transp. Porous Media* **23**, 1–30 (1996)

**Publisher's Note** Springer Nature remains neutral with regard to jurisdictional claims in published maps and institutional affiliations.